CHAPTER 6

Time Delay, Plant Uncertainty, and Robust Stability

Stability **A system is stable if all the poles are in the left half of the complex plane.**

Time delay system **is an infinite dimensional system, which means the system has infinite number of poles.**

How to make sure that all the infinite number of poles of the system are in the left half of the complex plane?

There was no solution to this important practical problem until 1932 when Harry Nyquist (1889 – 1976) developed the the Nyquist stability criterion based on Cauchy complex integral theorem presented by a French mathematician Augustin-Louis Cauchy (1789 –1857) in 1831.

6.1.1 Time Delay and Stability

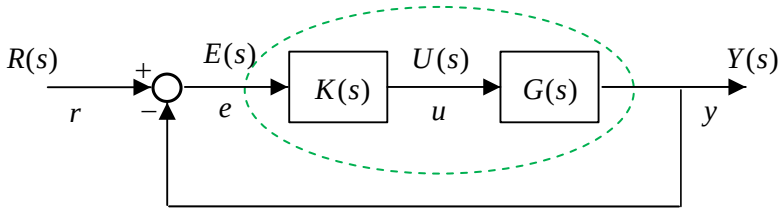

*Fig.*1

If the loop transfer function $L(s)$ is given as

$$L(s) = G(s)K(s) = \frac{2}{s+1}$$

then the closed-loop characteristic equation will be

$$1 + L(s) = 1 + \frac{2}{s+1} = 0 \quad \rightarrow \quad s + 3 = 0$$

Now, assume the delay time is *T*. Then the loop transfer function will become

$$L(s) = \frac{2}{s+1} e^{-sT}$$

where the term e^{-sT} is the transfer function of a time delay element with delay time *T*. The closed-loop characteristic equation will turn out to be

$$F(s) = 1 + L(s) = \frac{1}{s+1}\left[3 + (1-2T)s + T^2 s^2 - \frac{1}{3}T^3 s^3 + \cdots\cdots\right] = 0$$

which apparently is a polynomial equation with infinite numbers of roots.

6.1.2 Plant Uncertainty and Stability

A feedback control system usually is designed based on a mathmatical model of the system to be controlled, which is called the plant.

In practice, the real system to be controlled is not identical to theideal plant model due to unmodelled plant dynamics, specification tolerance of components, and plant parameter perturbations influenced by the environment conditions

Hence, a feedback control system not only needs to be stable for the nominal system with the ideal plant model, it should be designed to achieve robust stability against all possible plant uncertainties.

The Nyquist approach not only resolves the stability analysis issue of infinite-dimensional feedback control systems, it also provides important concepts and tools for achieving robust stability of feedback control systems.

6.2 Contour Mapping and Cauchy's Principle of the Argument

Ex 0: A Simple Real Function Mapping

Consider the simple real function

$$y = f(x) = -x + 2$$

x	-1	0	1	2	3
y	3	2	1	0	-1

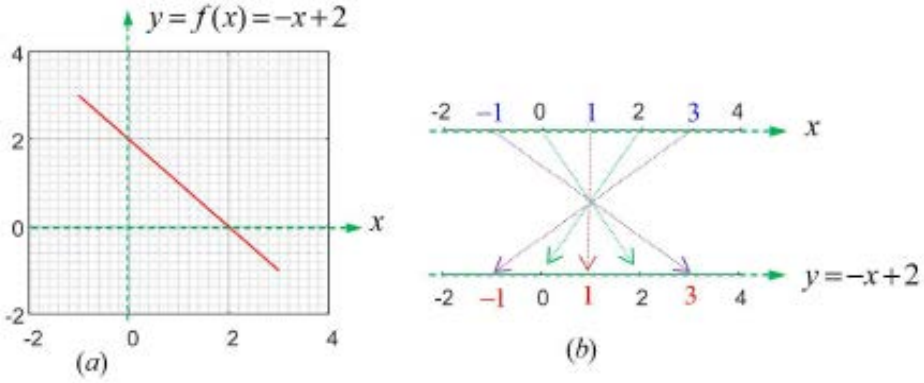

Fig. 2

Ex 1: An Illustration of Complex Function Contour Mapping

Consider the simple complex function

$$F(s) = \frac{s - 0.5}{s + 0.5}$$

How the *complex variable* s will affect the value of the *complex function* $F(s)$?

Assume s is moving along the simple closed contour Γ_s : $s = j\omega$, where $\omega = -1 \to 0 \to 1$, and then $s = e^{j\phi}$, where $\phi = \pi / 2 \to 0 \to -\pi / 2$.

The $F(s)$ mappings of segments (1) and (2), respectively, will be

$$F(j\omega)=\frac{j\omega-0.5}{j\omega+0.5}=\frac{e^{j(\pi-\theta)}}{e^{j\theta}}=e^{j(\pi-2\theta)},\quad \text{where}\quad \theta=\tan^{-1}\frac{\omega}{0.5},\quad \omega=-1\to 0\to 1$$

and

$$F(e^{j\phi})=\frac{e^{j\phi}-0.5}{e^{j\phi}+0.5}=\frac{0.75+j\sin\phi}{(\cos\phi+0.5)^2+\sin^2\phi},\quad \text{where}\quad \phi=\frac{\pi}{2}\to 0\to\frac{-\pi}{2}$$

The mapping relationship between s and $F(s)$ can be represented by the following tabulated chart:

s	$-j$	$\to$	$-j0.5$	$\to$	0	$\to$	$j0.5$	$\to$	j	$\to$	e^{j0}
$F(s)$	e^{-j53°	$\to$	$e^{-j\pi/2}$	$\to$	-1	$\to$	$e^{j\pi/2}$	$\to$	e^{j53°	$\to$	$1/3$

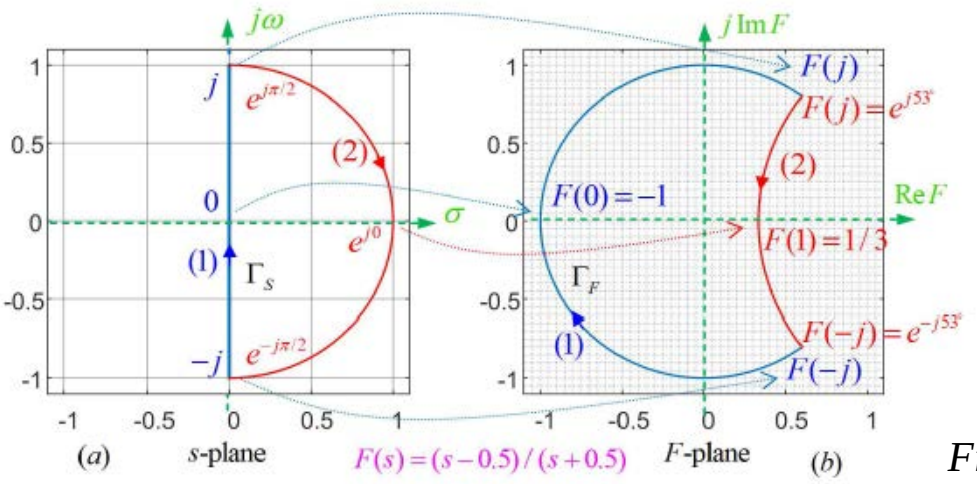

Fig. 3

After obtaining the complex contour mapping Γ_F, we are particularly interested in the number and direction of the encirclements of the origin by Γ_F on the F-plane.

It can be seen that Γ_F encircles the origin once clockwise, which is in the same direction of the Γ_s contour in the s-plane. Therefore, the number of encirclement is N = 1.

6.2.2 Cauchy's Principle of the Argument

Theorem 1: Cauchy's Principle of the Argument

Let Γ_s ***be a simple closed curve in the (complex) s-plane, as shown in the left graph of Figure 3.***

F(s) is a rational function having no poles or zeros on Γ_s***. Let*** Γ_F ***be the image of*** Γ_s ***under the map F(s). Then,***

$$N = Z - P$$

N *is the number of clockwise encirclements of the origin by* Γ_F *as s traverses* Γ_s *once in the clockwise direction;*

Z *is the number of zeros of F(s) enclosed by* Γ_s*, counting multiplicities; and*

P *is the number of poles of F(s) enclosed by* Γ_s*, counting multiplicities*

Proof:

$$F(s) = K\frac{(s-z_1)(s-z_2)\cdots(s-z_m)}{(s-p_1)(s-p_2)\cdots(s-p_n)}$$

$$F(s) = K\frac{\rho_{z1}e^{j\theta_{z1}}\rho_{z2}e^{j\theta_{z2}}\cdots\rho_{zm}e^{j\theta_{zm}}}{\rho_{p1}e^{j\theta_{p1}}\rho_{p2}e^{j\theta_{p2}}\cdots\rho_{pn}e^{j\theta_{pn}}} = \frac{K\rho_{z1}\rho_{z2}\cdots\rho_{zm}}{\rho_{p1}\rho_{p2}\cdots\rho_{pn}}e^{j[(\theta_{z1}+\theta_{z2}+\cdots+\theta_{zm})-(\theta_{p1}+\theta_{p2}+\cdots+\theta_{pn})]} \quad (*)$$

where

$$\rho_{zi} = |s-z_i|, \quad i = 1,\cdots,m \quad \text{and} \quad \rho_{pj} = |s-p_j|, \quad j = 1,\cdots,n$$
$$\theta_{zi} = \angle(s-z_i), \quad i = 1,\cdots,m \quad \text{and} \quad \theta_{pj} = \angle(s-p_j), \quad j = 1,\cdots,n$$

In view of Equation (*), as *s* traverses Γ_s **once, its image** Γ_F **encircles the origin only if at least one of the angles** θ_j **undergoes a change of** 2π **radians. Any pole or zero outside of** Γ_s **does not produce any angle change through a circuit of** Γ_s**. On the other hand, a pole or zero inside of** Γ_s **does produce a** 2π **angle change. Equation (*) implies that for a complete clockwise transverse of** Γ_s**, each zero inside of** Γ_s **produces a clockwise** 2π **angle change and each pole inside of** Γ_s **produces a counterclockwise** 2π **angle change. Hence, the net number of clockwise encirclements of the origin by** Γ_F **is** $Z - P$**.**

Ex 2: Illustration of the Principle of the Argument

Consider the complex rational function

$$F(s)=\frac{s-z_1}{(s-p_1)(s-p_2)(s-p_3)}=\frac{s-1}{(s+1-j)(s+1-j)(s-3)}=\frac{s-1}{s^3-s^2-4s-6}$$

and the simple closed path Γ_s is a circle centered at the origin of the *s*-plane with radius equals to 2. For clarity, Γ_s is partitioned into two segments:

Segment (1) is in red, which starts from $s=2$, clockwise along the semicircle to $s=2e^{-j135^\circ}$ and ends at $s=-2$.

Immediately, segment (2), which is in blue, begins from $s=-2$, moving along the upper semicircle to go back to $s=2$ to complete one revolution of the circle.

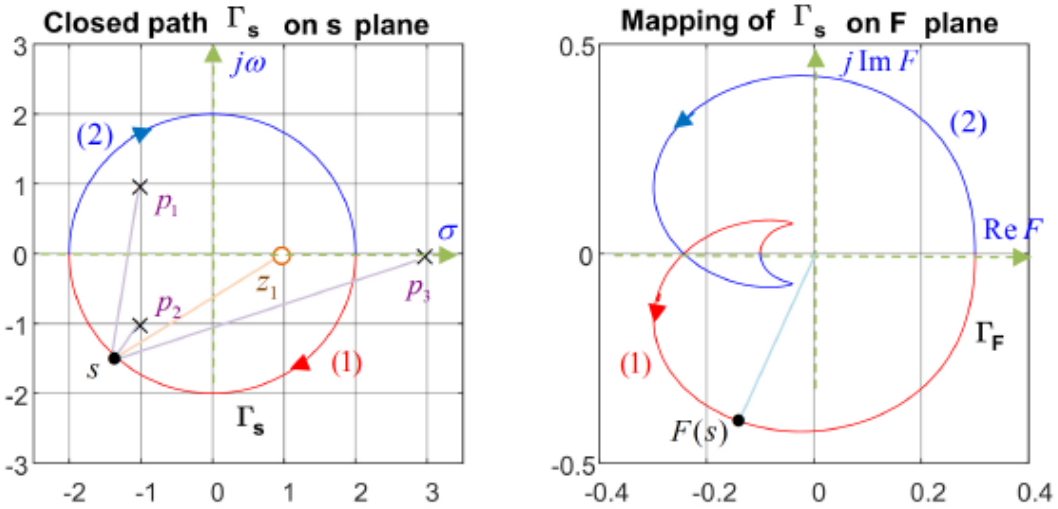

Fig. 4

The image of segment (1) of Γ_s is shown in the right graph of *Fig.* 4 as segment (1) of Γ_F, also in red. It can be seen that the starting point $s=2$ is mapped to $F(2)=-0.1$, $s=2e^{-j135^\circ}$ to $F(2e^{-j135^\circ})=-0.16212-j0.38819$, and $s=-2$ finds its image at $F(-2)=0.3$ on Γ_F.

Similarly, the three points on segment (2) of Γ_s: $s=-2$, $s=2e^{j135^\circ}$, and $s=2$ are mapped to $F(-2)=0.3$, $F(2e^{j135^\circ})=-0.16212+j0.38819$, and $F(2)=-0.1$, respectively, on Γ_F.

Note that Γ_s is symmetrical with respect to the real axis, and it encircles the origin of the *F*-plane once counterclockwise. Hence, the number of clockwise encirclements of the origin by Γ_F is $N=-1$.

Recall that the number of poles of $F(s)$ enclosed by Γ_s is $P=2$, and the number of zeros of $F(s)$ enclosed by Γ_s is $Z=1$.

Therefore, $N=-1=Z-P=1-2$, which is consistent with the result of Theorem 1.

Ex 3: A Pole or Zero Outside Γ_s Does Not Affect the Encirclement Number N, but Will Change the Shape of Contour Mapping Γ_F

The complex rational function $F(s)$ here is almost the same as that considered in the previous example, except that the pole p3 outside Γ_s is removed. That is,

$$F(s)=\frac{s-z_1}{(s-p_1)(s-p_2)}=\frac{s-1}{(s+1-j)(s+1-j)}=\frac{s-1}{s^2+2s+2}$$

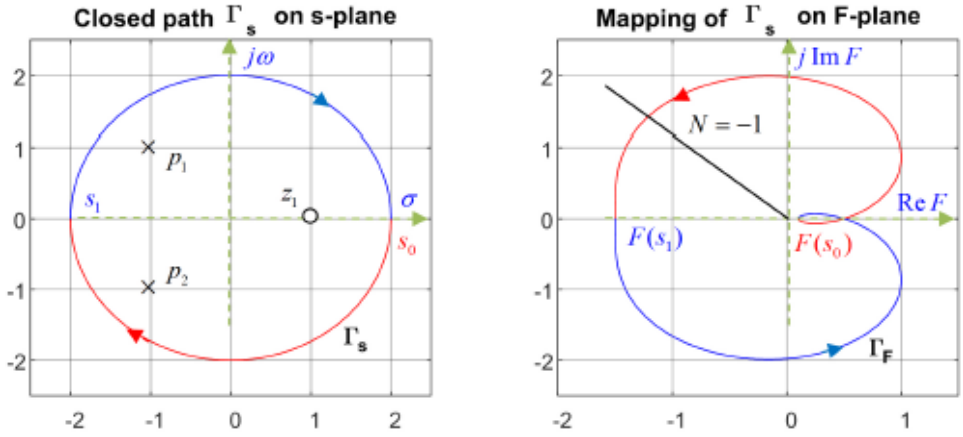

Fig. 5

The simple closed path Γ_s is still the same, which is a circle centered at the origin of the *s*-plane with radius equal to 2.

The image of segment (1) of Γ_s is shown in the right graph of *Fig.* 5 as segment (1) of Γ_F, also in red. It can be seen that the starting point $s=2$ is

mapped to $F(2)=0.1$, $s=-j2$ **to** $F(2e^{-j90^\circ})=0.5$, **and** $s=2e^{-j136.4^\circ}$ **to** $F(2e^{-j136.4^\circ})=j1.978$, **and** $s=-2$ **finds its image at** $F(-2)=-1.5$ **on** Γ_F.

Similarly, the four points on segment (2) of Γ_s: $s=-2$, $s=2e^{j136.4^\circ}$, $s=j2$, **and** $s=2$ **are mapped to** $F(-2)=-1.5$, $F(2e^{j136.4^\circ})=-j1.978$, $F(j2)=F(2e^{-j90^\circ})=0.5$ **and** $F(2)=0.1$, **respectively, on** Γ_F.

Note that Γ_F **is symmetrical with respect to the real axis, and it encircles the origin of the *F*-plane once, counterclockwise. Hence, the number of clockwise encirclements of the origin by** Γ_F **is** $N=-1$. **Recall that the number of poles of** $F(s)$ **enclosed by** Γ_s **is** $P=2$, **and the number of zeros of** $F(s)$ **enclosed by** Γ_s, **is** $Z=1$. **Therefore,** $N=-1=Z-P=1-2$, **which is consistent with the result of Theorem 1.**

Note that the *N*, *Z*, and *P* numbers are the same as those in Example 2, but the shape of contour mapping Γ_F **is very different from that in Example 2.**

In the next example, we will observe how the contour mapping Γ_F **and its clockwise encirclement number around the origin will be affected if the zero,** z_1, **inside** Γ_s **is removed.**

Ex 4: A Change of the Number of Poles or Zeros Inside Γ_s Will Affect the Encirclement Number *N* of Γ_F Around the Origin)

The complex rational function $F(s)$ **here is almost the same as that considered in the previous example, except that the zero** z_1 **inside** Γ_s **is removed. That is,**

$$F(s)=\frac{1}{(s-p_1)(s-p_2)}=\frac{1}{(s+1-j)(s+1-j)}=\frac{1}{s^2+2s+2}$$

The simple closed path Γ_s is still the same, which is a circle centered at the origin of the s-plane with radius equal to 2.

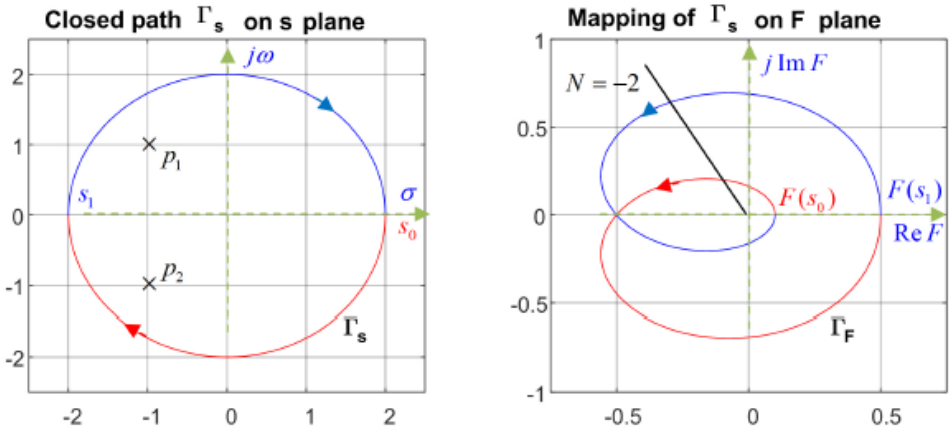

Fig. 6

The image of segment (1) of Γ_s is shown in the right graph of *Fig.* 6 as segment (1) of Γ_F, also in red. It can be seen that the starting point $s=2$ is mapped to $F(2)=0.1$, $s=-j2$ to $F(2e^{-j90^\circ})=0.1+j0.2$, $s=2e^{-j120^\circ}$ to $F(2e^{-j120^\circ})=-0.5$, and $s=2e^{-j144^\circ}$ to $F(2e^{-j144^\circ})=-j0.688$, and $s=-2$ finds its image at $F(-2)=0.5$ on Γ_F.

Similarly, the image of segment (2) of Γ_s can be found as the conjugate of the image of segment (1), as shown in the right graph of *Fig.* 6.

Note that Γ_F is symmetrical with respect to the real axis, and it encircles the origin of the *F*-plane twice, counterclockwise. Hence, the number of clockwise encirclements of the origin by Γ_F is $N=-2$.

Recall that the number of poles of $F(s)$ enclosed by Γ_s is $P=2$, and the number of zeros of $F(s)$ enclosed by Γ_s is $Z=0$.
Therefore, $N=-2=Z-P=0-2$, which is consistent with the result of Theorem 1.

6.3 Nyquist Path, Nyquist Plot, and Nyquist Stability Criterion

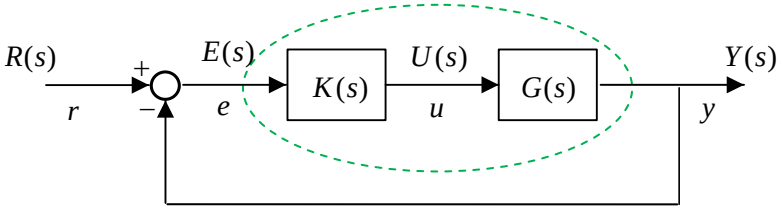

Fig. 7

The closed-loop system characteristic equation is

$$1 + L(s) = 0$$

where $L(s) = G(s)K(s)$ **is the loop transfer function. The closed-loop system is stable if and only if all the roots of the characteristic equation are in the strictly left half of the complex plane. One way to check the stability of the closed-loop system is to solve the equation for all the roots. This approach may become tedious or even impossible if the equation is of high order or has infinite number of roots.**

As described in Sec. 6.1.1, a system with time delay is an infinite-dimensional system whose characteristic equation has an infinite number of roots.

6.3.1 Nyquist Path

The Nyquist stability analysis approach provides an alternative way to check the closed-loop system stability without the need of finding the roots of the characteristic equation.

The tool Nyquist employed to solve the very important engineering problem was the Cauchy complex integral theorem or Cauchy's principle of the argument.

Nyquist's contributions:

(1) Create a special simple closed path Γ_s, now called Nyquist path or Nyquist contour, to enclose the entire right half of the complex plane;

(2) Define the mapping function

$$F(s) = 1 + L(s)$$

so that the zeros of $F(s)$ are the closed-loop system poles.

The Nyquist path is a simple closed path Γ_s that encloses the entire right half of the complex *s*-plane as shown in *Fig*. 8.

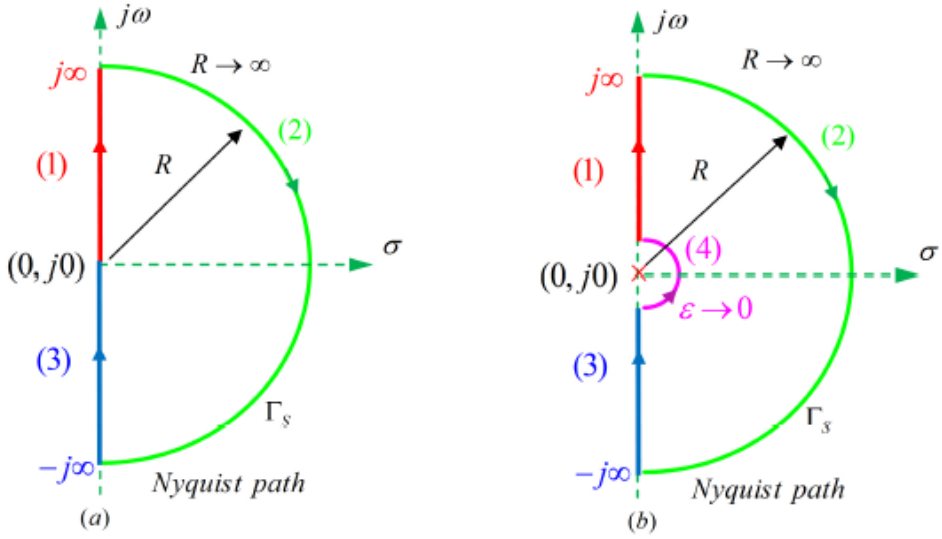

Fig. 8

The mapping function $F(s)$, which is the closed-loop characteristic function, is assumed to have no poles or zeros on Γ_s.

If $F(s)$ has a pole on the imaginary axis of the *s*-plane, a tiny semicircle contour with radius ε will be employed to go around it, as shown in *Fig*. 8(b).

If $F(s)$ has no poles on the imaginary axis, the Nyquist path Γ_s will look like the one shown in *Fig*. 8(a). For clarity, the Nyquist path is divided into the following three segments:

1: Segment (1) starts from the origin of the s-plane, moving up on the imaginary axis with $s = j\omega$, $\omega = 0 \to \infty$.

2: Segment (2) is a huge semicircle with $s = \lim_{R\to\infty} Re^{j\phi}$ and $\phi = 90^\circ \to 0^\circ \to -90^\circ$.

3: Segment (3) is the complex conjugate of Segment (1), which starts from $s = -j\infty$, moving up on the imaginary axis back to the origin of the s-plane (i.e., $s = j\omega$, $\omega = -\infty \to 0$).

In the case that $F(s)$ has a pole at the origin, as shown in *Fig*. 8(b), the Nyquist path Γ_s will have four segments with a tiny semicircle segment (4) inserted between segments (3) and (1):

1: Segment (1) starts from $s = j\varepsilon$, moving up on the imaginary axis with $s = j\omega$, $\omega = \varepsilon \to \infty$.

2: Segment (2) is a huge semicircle with $s = \lim_{R\to\infty} Re^{j\phi}$ and $\phi = 90^\circ \to 0^\circ \to -90^\circ$.

3: Segment (3) is the complex conjugate of segment (1), which starts from $s = -j\infty$, moving up on the imaginary axis with $s = j\omega$, $\omega = -\infty \to -\varepsilon$.

4: Segment (4) is a tiny semicircle with $s = \lim_{\varepsilon\to 0} \varepsilon e^{j\phi}$ and $\phi = -90^\circ \to 0^\circ \to 90^\circ$.

6.3.2 Nyquist Plot

An $F(s)$ mapping of the Nyquist path Γ_s can be produced as Γ_F on another complex plane, the $F(s)$-plane.

This Γ_F plot is called the Nyquist plot of $F(s)$.

Then, according to Cauchy's principle of the argument in Theorem 1, we have $N = Z - P$, where N is the number of clockwise encirclements of the origin by Γ_F, and Z and P are the numbers of zeros and poles of $F(s)$ enclosed by Γ_s in the *s*-plane.

Since $F(s)$ and the loop transfer function $L(s)$ share the same poles, P is the number of the poles of $L(s)$ in the right half of the *s*-plane, which is usually given or can be easily computed. The encirclement number N can be counted from Γ_F, the Nyquist plot of $F(s)$.

Therefore, we will have $Z = N + P$, which is the number of zeros of $F(s)$ enclosed by Γ_s, or, equivalently, the number of the closed-loop system poles in the right half of *s*-plane.

The closed-loop system is stable if and only if $Z = 0$.

Ex 5:

Construction of Nyquist Plot of $F(s)$ for a Simple Feedback Control System

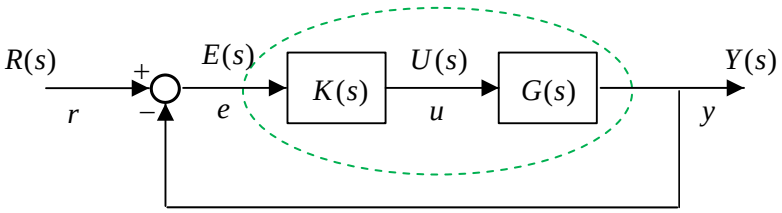

Fig. 7

Consider the feedback control system shown in *Fig*.7, where the loop transfer function $L(s)$ and the characteristic function $F(s)$ of the closed-loop system are given as

$$L(s) = 2\frac{s-1}{s+1} \quad \rightarrow \quad F(s) = 1 + L(s) = \frac{3s-1}{s+1}.$$

It is easy to see that $F(s)$ has one zero, $s = 1/3$, in the right half of *s*-plane and, therefore the closed-loop system is unstable.

However, we will employ this simple example to demonstrate how to use the Nyquist approach to determine the number of zeros of $F(s)$ enclosed by the Nyquist path Γ_s.

Since $F(s)=1+L(s)$, we will construct Γ_L, the Nyquist plot of $L(s)$ first, and then shift the graph of Γ_L to the right by one unit to obtain the Nyquist plot of $F(s)$. The procedure for constructing Γ_L, the Nyquist plot of $L(s)$, is given as follows:

1: On segment (1) of the Nyquist path Γ_s, we have $s = j\omega$, and $\omega = 0 \to 1 \to \infty$. Then the trajectory of

$$L(j\omega) = 2\frac{j\omega - 1}{j\omega + 1} = 2\frac{\sqrt{\omega^2+1}\, e^{j(\pi-\theta)}}{\sqrt{\omega^2+1}\, e^{j\theta}} = 2e^{j(\pi-2\theta)} \quad \text{where} \quad \theta = \tan^{-1}\omega \tag{9.16}$$

will be a red upper semicircle, shown in Figure 9(b), with radius equal to 2, starting from $L(j0) = 2e^{j\pi}$ to $L(j1) = 2e^{j\pi/2}$ and ending at $L(j\infty) = 2$.

2: Segment (2) is a huge semicircle with $s = \lim_{R\to\infty} Re^{j\phi}$ and $\phi = 90^\circ \to 0^\circ \to -90^\circ$. With $s = Re^{j\phi}$, we have

$$\lim_{R\to\infty} L(Re^{j\phi}) = \lim_{R\to\infty} 2\frac{Re^{j\phi} - 1}{Re^{j\phi} + 1} = 2 \tag{9.17}$$

hence, the entire segment (2) semicircle is mapped to the single point $(2, j0)$ on L-plane indicated by a green dot in Figure 9(b).

3: The image of segment (3) is the blue lower semicircle with radius equal to 2, starting from $L(-j\infty) = 2$ to $L(-j1) = 2e^{-j\pi/2}$ and ending at $L(j0) = -2$, which is the complex conjugate of the image of segment (1).

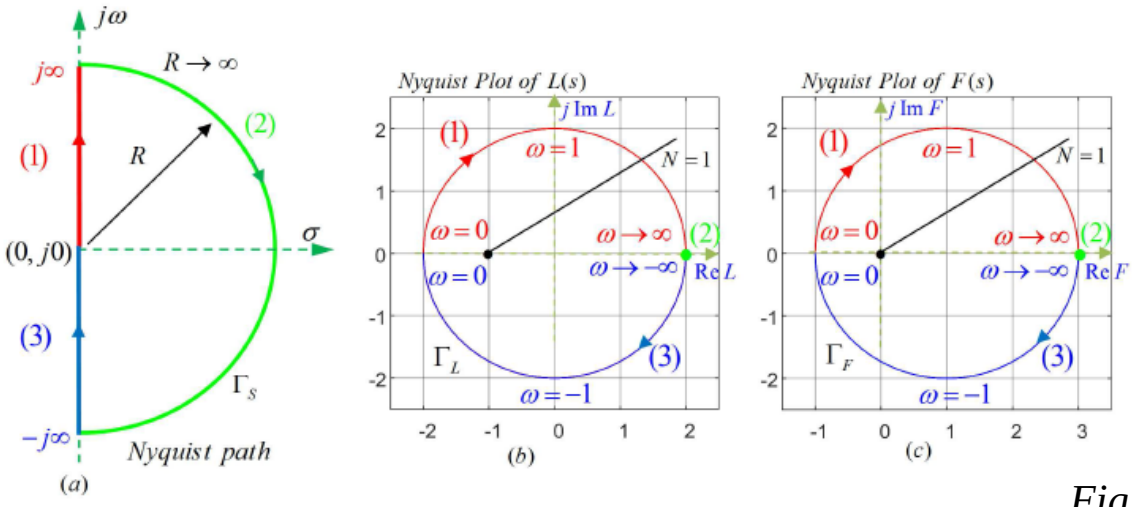

Fig. 9

Remark:
The number of encirclements of the origin $(0, j0)$ by Γ_F equals to that of the critical point $(-1, j0)$ by Γ_L.

From now on, we will just employ the Nyquist plot of $L(s)$, Γ_L, together with the critical point $(-1, j0)$ to determine the stability of the closed-loop system.

6.3.3 Nyquist Stability Criterion

Theorem 2: Nyquist Stability Criterion Theorem

Suppose the s-plane Nyquist contour Γ_s has an image in the L-plane that encircles the critical point $(-1, j0)$ clockwise N times. Moreover, suppose there are P poles of $L(s)$ in the right half s-plane.

Then the number of unstable closed-loop system poles is $Z = N + P$ since $N = Z - P$, as shown in Theorem 1, Cauchy's principle of the argument.

Remark:

Nyquist's theorem simply restates Cauchy's principle of the argument as

The number of closed-loop system poles in the RHP, Z, equals the number of clockwise encirclements of the $(-1, j0)$ point in the L-plane, N, plus the number of the loop transfer function poles in the RHP, P.

Ex 6:
Nyquist Plot of $L(s)$ with a Pole at the Origin and a Parameter K

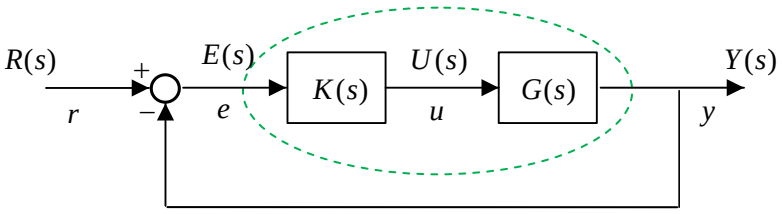

Fig. 7

Consider the feedback control system shown in *Fig.* 7, where the loop transfer function $L(s)$ and the characteristic function $F(s)$ of the closed-loop system are given as

$$L(s)=\frac{K(s-1)}{s(s+1)} \quad \text{and} \quad F(s)=1+L(s)=1+\frac{K(s-1)}{s(s+1)}=\frac{s^2+(K+1)s-K}{s(s+1)}$$

The closed-loop characteristic equation is

$$s^2+(K+1)s-K=0$$

According to Routh-Hurwitz stability criterion, the closed-loop system is stable if and only if the parameter *K* satisfies the following inequality:

$$K+1>0 \quad \text{and} \quad -K>0\,, \qquad \text{or equivalently,} \qquad -1<K<0$$

However, this example is here mainly to demonstrate how to construct the Nyquist plot of the loop transfer function $L(s)$ that has a pole at the origin and a design parameter *K*.

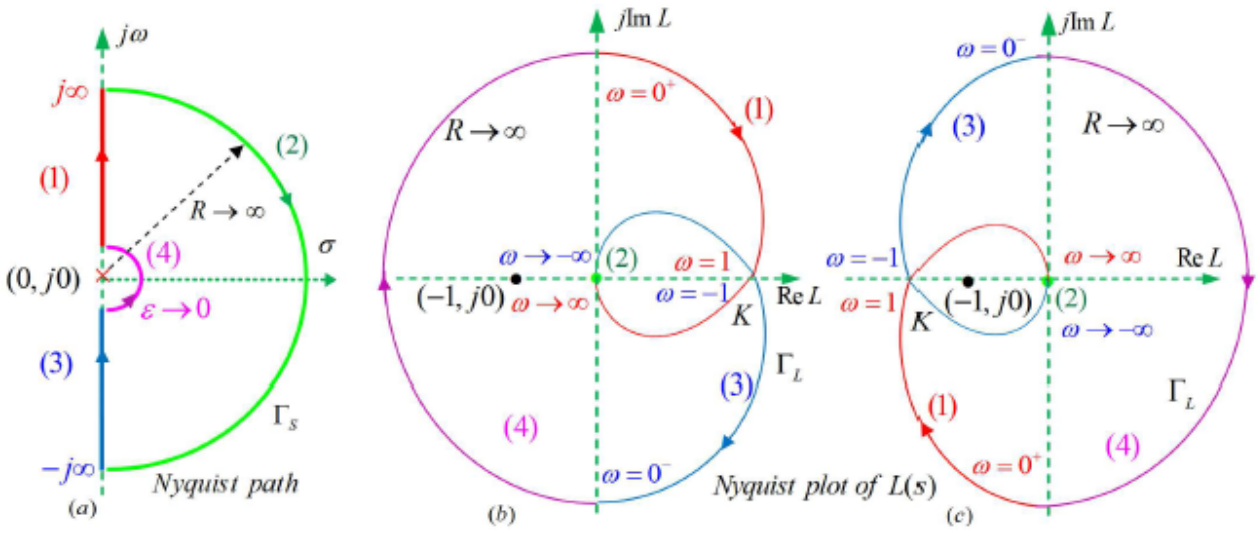

***Fig.* 10 Nyquist plot of $L(s)$: (b) when $K>0$, (c) when $K<0$**

The Nyquist plot of $L(s)$, Γ_L, will be used together with Theorem 2, the Nyquist stability criterion, to determine the number of closed-loop system poles in the RHP.

Note that the Nyquist path Γ_s shown in *Fig.*10(a) consists of four segments. Segment (4), a tiny semicircle with radius ε around the pole at the origin, is added to fulfill the assumption that Γ_s should not have poles on it.

The procedure to constructing Γ_L, with $K > 0$, is given as follows:

1: On segment (1) of the Nyquist path Γ_s, the variable $s = j\omega$, is assumed to be moving along the imaginary axis following $\omega = \varepsilon \to 1 \to \infty$. The corresponding image on L-plane, Γ_L, will be

$$L(j\omega) = \frac{K(j\omega - 1)}{j\omega(j\omega + 1)} = \frac{K\sqrt{\omega^2+1}\, e^{j(\pi-\theta)}}{\omega\sqrt{\omega^2+1}\, e^{j\pi/2}e^{j\theta}} = \frac{K}{\omega}e^{j(\pi/2-2\theta)} \quad \text{where} \quad \theta = \tan^{-1}\omega \tag{9.19}$$

which is in red with label (1) passing through the following three points:

$$L(j\varepsilon) = \lim_{\varepsilon\to 0}\frac{K}{\varepsilon}e^{j\pi/2} = \infty e^{j\pi/2} \to L(j1) = K \to L(jR) = \lim_{R\to\infty}(\frac{K}{R})e^{-j\pi/2} = 0e^{-j\pi/2} \tag{9.20}$$

Note that $L(j1) = K > 0$ means that when $\omega = 1$ rad/s, segment (1) of the Nyquist image Γ_L intersects the real axis of the L-plane at $(K, j0)$, as shown in Figure 9.10(b).

2: Segment (2) is a huge semicircle, with $s = \lim_{R\to\infty} Re^{j\phi}$ and $\phi = \pi/2 \to 0 \to -\pi/2$. With $s = Re^{j\phi}$, we have

$$\lim_{R\to\infty} L(Re^{j\phi}) = \lim_{R\to\infty}\frac{K(Re^{j\phi}-1)}{Re^{j\phi}(Re^{j\phi}+1)} = \lim_{R\to\infty}\frac{K}{R}e^{-j\phi} = 0e^{-j\phi}, \quad \text{where} \quad -\phi = \frac{-\pi}{2} \to 0 \to \frac{\pi}{2} \tag{9.21}$$

hence, **the entire segment (2) semicircle is mapped to the single point $(0, j0)$ on the L-plane**, indicated by a green dot in Figure 9.10(b).

3: The image of segment (3) is in blue with label (3) passing through the following three points:

$$L(-jR) = \lim_{R\to\infty}\frac{K}{R}e^{j\pi/2} = 0e^{j\pi/2} \to L(-j1) = K \to L(-j\varepsilon) = \lim_{\varepsilon\to 0}\frac{K}{\varepsilon}e^{-j\pi/2} = \infty e^{-j\pi/2} \tag{9.22}$$

4: **Segment (4) is a tiny semicircle with $s = \lim_{\varepsilon\to 0}\varepsilon e^{j\psi}$ and $\psi = -\pi/2 \to 0 \to \pi/2$.** With $s = \varepsilon e^{j\psi}$ and $\psi = -\pi/2 \to 0 \to \pi/2$, we have

$$\lim_{\varepsilon\to 0} L(\varepsilon e^{j\psi}) = \lim_{\varepsilon\to 0}\frac{K(\varepsilon e^{j\psi}-1)}{\varepsilon e^{j\psi}(\varepsilon e^{j\psi}+1)} = \lim_{\varepsilon\to 0}\frac{K}{\varepsilon}e^{j(\pi-\psi)} = \infty e^{j(\pi-\psi)} \quad \text{where} \quad \pi - \psi = \frac{3\pi}{2} \to \pi \to \frac{\pi}{2} \tag{9.23}$$

hence, the tiny semicircle, segment (4), is mapped to the huge semicircle with radius $R \to \infty$ passing through the following three points on the L-plane:

$$L(\varepsilon e^{-j\pi/2}) = \infty e^{j3\pi/2} \to L(\varepsilon e^{j0}) = \infty e^{j\pi} \to L(\varepsilon e^{j\pi/2}) = \infty e^{j\pi/2} \tag{9.24}$$

Now we have the Nyquist plot of $L(s)$, Γ_L, on the *L*-plane, as shown in *Fig.* 10(b) for the case with $K > 0$. The number of clockwise encirclements of the critical point $(-1, j0)$ by the Nyquist plot Γ_L is $N = 1$.

Meanwhile, the number of the poles of $L(s)$ enclosed by Γ_s is $P = 0$. Hence, according to Nyquist stability criterion, $Z = N + P = 1+0 = 1$, which implies that the closed-loop system has one pole in the RHP; therefore, the closed-loop system is unstable.

For the case with $K < 0$, the Nyquist plot of $L(s)$, Γ_L, is shown in *Fig.*10(c). Notice that the number N of clockwise encirclements of $(-1, j0)$ by the Nyquist plot Γ_L is dependent on the intersection of Γ_L with the real axis. If the intersection point is between $(-1, j0)$ and $(0, j0)$, or, equivalently, $-1 < K < 0$, the encirclement number is $N = 0$.

Hence, according to Nyquist stability criterion, $Z = N + P = 0+0 = 0$, which implies that the closed-loop system has no pole in the RHP; therefore, the closed-loop system is stable when $-1 < K < 0$.

Ex 7: Nyquist Plot of $L(s)$ with a Pole in RHP and a Parameter K

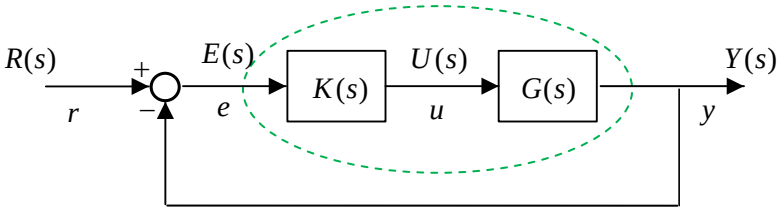

Fig. 7

Assume the loop transfer function $L(s)$ is given as

$$L(s) = \frac{0.6K}{(s-0.5)(s^2+s+1)}$$

Then we have the characteristic function F(s) of the closed-loop system as

$$F(s) = 1 + L(s) = 1 + \frac{0.6K}{(s-0.5)(s^2+s+1)} = \frac{s^3+0.5s^2+0.5s+0.6K-0.5}{(s-0.5)(s^2+s+1)}$$

Note that the loop transfer function $L(s)$ has a pole in the RHP and a design parameter *K*, which is to be determined so that the closed-loop system is stable.

The Nyquist stability analysis approach will be employed to achieve the objective.

The procedure to constructing Γ_L, the Nyquist plot of $L(s)$ with *K* = 1.3, is given as follows:

1: On segment (1) of the Nyquist path Γ_s, the variable $s = j\omega$, is assumed to move along the imaginary axis following $\omega = 0 \to 0.707 \to \infty$. Then, the trajectory of

$$L(j\omega) = \frac{0.6K}{(j\omega - 0.5)(-\omega^2 + j\omega + 1)} = 0.6K \frac{-0.5(\omega^2+1) + j\omega(\omega^2 - 0.5)}{(0.5^2 + \omega^2)((\omega^2-1)^2 + \omega^2)} \tag{9.26}$$

will be a solid green curve labeled as (1), shown in Figure 9.11(b), starting from $L(j0) = -1.2K = -1.56$ to $L(j0.707) = -0.8K = -1.04$ and ending at $L(j\infty) = 0$. Note that segment (1) of the Nyquist plot Γ_L with $K = 1.3$, the solid green curve, intersects the negative real axis of the L-plane at these three points.

2: Segment (2) is a huge semicircle of Γ_s, with $s = \lim_{R\to\infty} Re^{j\phi}$ and $\phi = \pi/2 \to 0 \to -\pi/2$. With $s = Re^{j\phi}$, we have

$$\lim_{R\to\infty} L(\mathrm{Re}^{j\phi}) = \lim_{R\to\infty} \frac{0.6K}{(\mathrm{Re}^{j\phi} - 0.5)(R^2 e^{j2\phi} + \mathrm{Re}^{j\phi} + 1)} = \lim_{R\to\infty} \frac{K}{R^3} e^{-j3\phi} = 0e^{-j3\phi} \tag{9.27}$$

where $-3\phi = \frac{\pi}{2} \to 0 \to \frac{-\pi}{2}$; hence, the entire segment (2) semicircle is mapped to the single point $(0, j0)$ on the L-plane, as shown in Figure 9.11(b).

3: The image of segment (3) with $K = 1.3$ is in dashed green with label (3) passing through the following three points:

$$L(-jR) = \lim_{R\to\infty} \frac{K}{R} e^{-j\pi/2} = 0e^{-j\pi/2} \begin{array}{l} \to L(-j0.707) = -0.8K = -1.04 \\ \to L(-j0) = -1.2K = -1.56 \end{array} \tag{9.28}$$

With three *K* values, we have three corresponding double-crossing Nyquist plots of $L(s)$, Γ_L, on the *L*-plane, as shown in *Fig*.11(b). Note that each Nyquist plot intersects with the negative axis twice.

The Nyquist plot in green is for the case with *K* = 1.3. The number of clockwise encirclements of the critical point $(-1, j0)$, marked as the black dot, by the Nyquist image Γ_L, is *N* = 1. Meanwhile, the number of the poles of $L(s)$ enclosed by Γ_s is *P* = 1. Hence, according to Nyquist stability criterion,

$Z = N + P = 1+1 = 2$, which implies that the closed-loop system has two poles in the RHP. Therefore, the closed-loop system is unstable when $K = 1.3$.

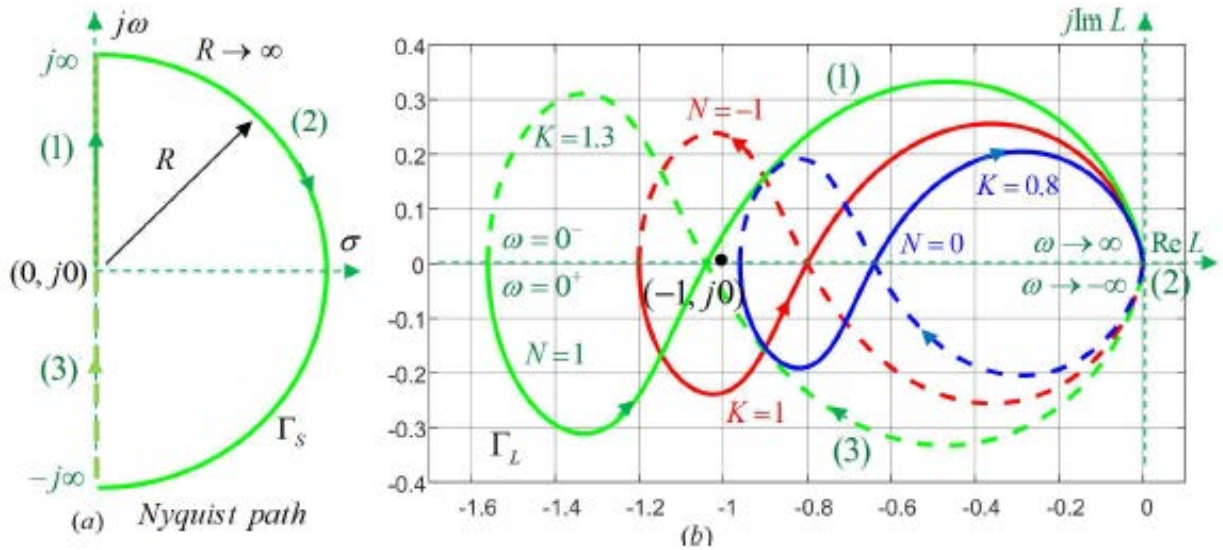

***Fig.* 11 Nyquist plot of $L(s)$ with an RHP pole and a parameter K for Ex. 7**

For the case with $K = 1$, this procedure can be repeated to obtain the Nyquist image of $L(s)$, Γ_L, as shown in *Fig.*11(b) in red labeled with $K = 1$. The red mapping contour intersects the real axis at the following three points:

$$L(j0) = -1.2K = -1.2\,, \quad L(\pm j0.707) = -0.8K = -0.8\,, \quad L(\pm j\infty) = 0$$

It also encircles the critical point $(-1, j0)$ once, counterclockwise; hence, the number of clockwise encirclement of $(-1, j0)$ by the red Γ_L is $N = -1$.

With $P = 1$, we have the number of unstable closed-loop system poles $Z = N + P = (-1) + 1 = 0$. Therefore, the closed-loop system is stable when $K = 1$.

The Nyquist plot of $L(s)$, Γ_L, associated with $K = 0.8$ is in blue, labeled with $K = 0.8$, as shown in *Fig.*11(b). The blue mapping contour intersects the real axis at the following three points:

$$L(j0) = -1.2K = -0.96, \quad L(\pm j0.707) = -0.8K = -0.64, \quad L(\pm j\infty) = 0$$

It does not encircle the critical point $(-1, j0)$, which implies $N = 0$. Thus, the number of unstable closed-loop system poles is one since $Z = N + P = 0 + 1 = 1$. Therefore the closed-loop system is unstable when $K = 0.8$.

Next, we would like to find the range of the design parameter *K* so that the closed-loop system is stable.

It is observed that the Nyquist plot Γ_L consists of two loops attaching together on the negative real axis at the $L=-0.8K$ intersection point. The right end of the right loop is always connected to the origin of the *L*-plane, but the left end of the left loop is $L=-1.2K$.

The encirclement direction of the left loop is counterclockwise, but the right loop is circling in the opposite direction. For the closed-loop system to be stable, the critical point $(-1, j0)$ has to be inside the left loop. Therefore, the closed-loop system is stable if and only if the following two inequalities are satisfied:

$$-1.2K < -1 \quad \text{and} \quad -1 < -0.8K$$

which is equivalent to

$$\frac{5}{6} < K < \frac{5}{4}$$

The intersection points of the Nyquist plot Γ_L with the real axis can be obtained from setting the imaginary part of Equation 9.26 to zero. That is,

$$\omega(\omega^2 - 0.5) = 0 \quad \rightarrow \quad \omega = 0 \quad \text{or} \quad \omega = \pm\sqrt{0.5} = \pm 0.707 \text{rad/s}$$

Then we have the two intersection points on the real axis at

$$L(j0) = 0.6K\frac{-0.5(0+1)}{(0.5^2+0)((0-1)^2+0)} = -1.2K$$

$$L(\pm j0.707) = 0.6K\frac{-0.5(0.5+1)}{(0.5^2+0.5)((0.5-1)^2+0.5)} = -0.8K$$

Furthermore, as $\omega \to \infty$, the Nyquist plot Γ_L will also intersect the real axis at the origin of the L-plane, since $L(\pm j\infty) = 0$. ■

6.3.4
Stability Issue Arising from Feedback Control System with Time Delay

Time delay in a feedback control system may lead to instability if the delay time is over some limit.

As discussed in Sec. 6.1.1, a system with time delay is an infinite-dimensional system with infinite number of poles.

The Nyquist stability criterion is capable of effectively counting the number of infinite-dimensional closed-loop system poles in the RHP without the need to compute all the poles.

In the following, the Nyquist stability analysis approach will be employed to investigate how the delay time T will affect the stability of the closed-loop system.

Ex 8: Nyquist Plot of $L(s)$ with a Time Delay Parameter T

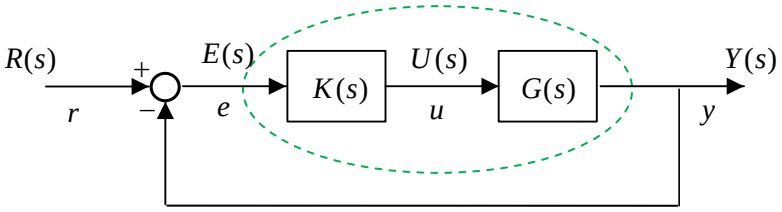

Fig. 7

The loop transfer function $L(s)$ and the characteristic function $F(s)$ of the closed-loop system are given as

$$L(s)=\frac{2e^{-sT}}{s+1},\quad F(s)=1+L(s)=\frac{1}{s+1}\left[3+(1-2T)s+T^2s^2-\frac{1}{3}T^3s^3+\cdots\cdots\right]$$

The procedure to constructing Γ_L, the Nyquist plot of $L(s)$ with delay time T = 1.0 s, is given as follows. We will see how the variation of T affects the performance of the closed-loop system after the Nyquist plot is completed.

1: On segment (1) of the Nyquist path Γ_s, the variable $s = j\omega$ is assumed to move along the imaginary axis following $\omega = 0 \to 2.029 \to \infty$. Then the trajectory of the mapped contour will be determined by the following equation:

$$L(j\omega) = \frac{2e^{-j\omega T}}{1+j\omega} = \frac{2}{\sqrt{1+\omega^2}\, e^{j\theta}} e^{-j\omega T} = \frac{2}{\sqrt{1+\omega^2}} e^{-j(\omega T+\theta)} \quad \text{where} \quad \theta = \tan^{-1}\omega \qquad (9.33)$$

This polar form complex function can also be written in the following rectangular form:

$$L(j\omega) = \frac{2}{\sqrt{1+\omega^2}} \cos(\omega T+\theta) - j\frac{2}{\sqrt{1+\omega^2}} \sin(\omega T+\theta) \quad \text{where} \quad \theta = \tan^{-1}\omega \qquad (9.34)$$

When ω increases from 0 to 4.913, the values of the complex function $L(j\omega)$ will change according to Equation 9.33 to generate the following tabulated chart:

ω	$0 \to 0.861 \to 2.029 \to 3.426 \to 4.913$
$\angle L(j\omega)$	$0 \to -\pi/2 \to -\pi \to -3\pi/2 \to -2\pi$
$\lvert L(j\omega)\rvert$	$2 \to 1.516 \to 0.884 \to 0.56 \to 0.399$

(9.35)

It starts from $L(j0) = 2$ and will spiral around the origin clockwise, with decreasing radius via the points $L(j0.861) = 1.516e^{-j\pi/2}$, $L(j2.029) = -0.884$, $L(j3.426) = 0.56e^{-j3\pi/2}$, to arrive at $L(j4.913) = 0.399e^{-j2\pi}$ to complete the first spiraling cycle. As ω continues to increase, the Nyquist plot Γ_L will spiral around the origin infinite times and approach the origin as $\omega \to \infty$. The trajectory is shown in red, labeled as (1), shown in Figure 9.12(b).

2: Segment (2) is a huge semicircle of Γ_s, with $s = \lim_{R\to\infty} Re^{j\phi}$ and $\phi = \pi/2 \to 0 \to -\pi/2$. With $s = Re^{j\phi}$, we have

$$\lim_{R\to\infty} L(Re^{j\phi}) = \frac{2}{\lim_{R\to\infty}\left(e^{RT(\cos\phi + j\sin\phi)}(Re^{j\phi}+1)\right)} = 0 \qquad (9.36)$$

hence, the entire segment (2) semicircle is mapped to the single point $(0, j0)$ on the L-plane, as shown in Figure 9.12(b).

3: The image of segment (3) is in blue with label (3), which is the conjugate of the image of segment (1). The red and the blue Γ_L trajectories are symmetrical with respect to the real axis.

Now we have the complete Nyquist plot of $L(s)$, Γ_L, for the system with delay time T = 1 s. Since the leftmost intersection point of Γ_L with the negative real axis is on the right-hand side of the critical point $(-1, j0)$, the number of clockwise encirclements of $(-1, j0)$, marked as the red dot, by the Nyquist image Γ_L, is N = 0.

Meanwhile, the number of the poles of $L(s)$ in the RHP is $P = 0$. Hence, according to Nyquist stability criterion, $Z = N + P = 0 + 0 = 0$, which implies that the closed-loop system has no poles in the RHP; therefore, the closed-loop system is stable when the delay time is $T = 1$s or less.

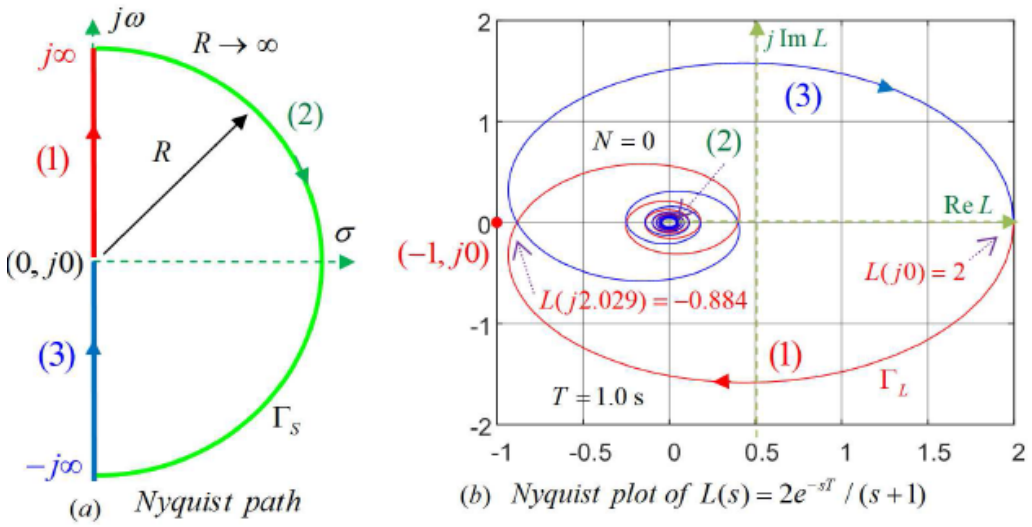

***Fig.* 12 Nyquist plot of $L(s)$ with a time delay T for Ex. 8**

Critical Delay Time

From the Nyquist plot graph Γ_L in *Fig.*12(b), it is observed that the leftmost intersection point of Γ_L will move to the left if the delay time T increases. Based on Equations 9.33 and 9.34, we will have $L(j\omega) = -1$, which means Γ_L intersects the real axis at $(-1, j0)$, if there exists a delay time T_c and a frequency ω_c so that the following two equations are satisfied:

$$\frac{2}{\sqrt{1+\omega_c^2}} = 1 \quad \text{and} \quad \omega_c T_c + \tan^{-1}\omega_c = \pi$$

The solution of the equations provides the smallest delay time that would destabilize the system:

$$\omega_c = \sqrt{3} = 1.732\,\text{rad/s} \quad \text{and} \quad T_c = \frac{2\pi}{3\sqrt{3}} = 1.209\,\text{s}$$

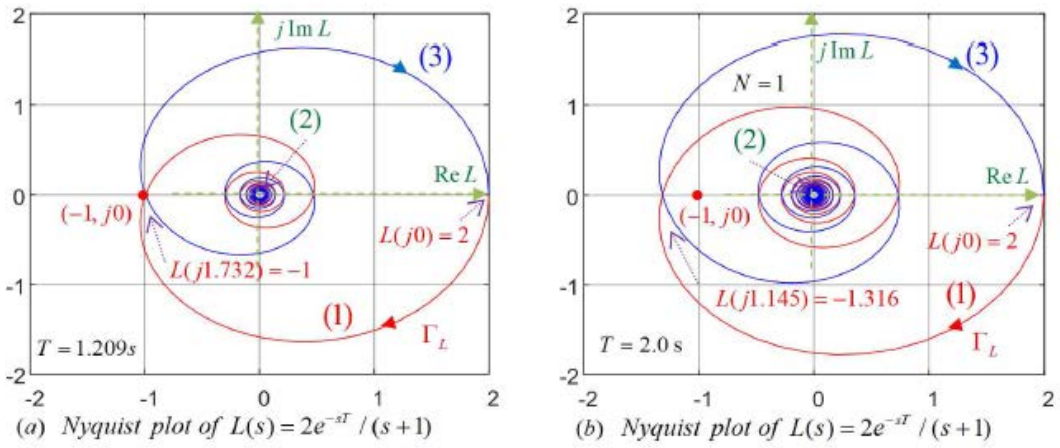

***Fig.* 13 Critical delay time that will destabilize the system.**

As shown in *Fig.*13(a), if the delay time is T = T_c = 1.209s, the Nyquist plot Γ_L trajectory will intersect the negative real axis at $(-1, j0)$ when $\omega = \omega_c = 1.732$ rad/s (i.e., $L(j1.732) = -1$).

If the delay time of the system is greater than the critical delay time, $T > T_c = 1.209$ s, the leftmost intersection point of Γ_L on the real axis will be on the left-hand side of $(-1, j0)$, as shown in *Fig.*13(b), and then the number of clockwise encirclements of $(-1, j0)$ by Γ_L will become *N* = 1. Hence, the number of closed-loop system poles in the RHP will be one since *Z = N + P* = 1 + 0 = 1 according to the Nyquist stability criterion. Therefore, the closed-loop system is unstable if the delay time *T* is greater than the critical delay time T_c = 1.209s.

Bode Plot Perspective

In Ex. 8, the Nyquist plot of the loop transfer function $L(s)$ and the Nyquist stability criterion were employed to investigate the stability issue caused by time delay in a feedback control system.

In the following example we will consider the same system regarding the same stability issue, but the main tool is the Bode plot instead of the Nyquist plot.

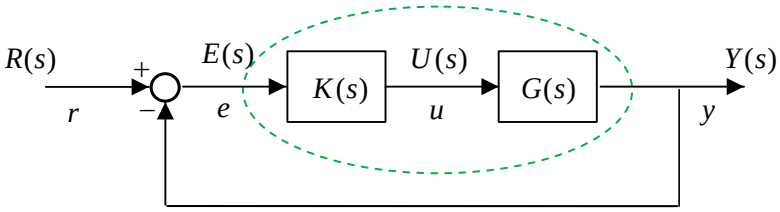

Fig. 7

The loop transfer function $L(s)$ **is** $L(s) = G(s)K(s)$.

The overall transfer function is $M(s) = \dfrac{L(s)}{1+L(s)} = \dfrac{Y(s)}{R(s)}$

Review of sinusoidal steady-state output response due to $r(t) = \cos\omega t$ **:**

$$y_{ss}(t) = A\cos(\omega t + \theta) \quad \text{where} \quad A = |M(j\omega)| \quad \text{and} \quad \theta = \angle M(j\omega)$$

Note that both the magnitude $|M(j\omega)|$ **and the phase** $\angle M(j\omega)$ **are functions of the frequency** ω**. When the frequency of the sinusoidal input signal varies, the amplitude and the phase of the steady-state sinusoidal response will change accordingly.**

The Bode plot consist of the magnitude and phase plots to explicitly exhibit their values at each frequency of interest.

Ex 9:
Bode Plot Perspective of the Stability Issues Caused by Time Delay

In addition to being an effective graphical display of the frequency response of a system, Bode plot are important tools for feedback control systems design.

However, in almost all feedback control systems design and analysis, we employ the loop transfer function $L(s)$ **instead of the closed-loop transfer function** $M(s)$ **in the design/analysis process. For the same reason, the Bode plot of the loop transfer function** $L(s)$ **(NOT the closed-loop transfer function** $M(s)$**) will be constructed to determine the stability margins of the closed-loop system.**

For the loop transfer function of a system with time delay *T*,

$$L(s) = \frac{2e^{-sT}}{s+1}$$

$L(j\omega)$ can be expressed in polar form as:

$$L(j\omega) = \frac{2e^{-j\omega T}}{1+j\omega} = \frac{2}{\sqrt{1+\omega^2}\,e^{j\theta}}e^{-j\omega T} = \frac{2}{\sqrt{1+\omega^2}}e^{-j(\omega T+\theta)}, \quad \text{where} \quad \theta = \tan^{-1}\omega$$

Then we have the magnitude and the phase of $L(j\omega)$ in dB and degree, respectively, as functions of frequency in rad/s in the following:

$$|L(j\omega)|_{dB} = 20\log_{10}|L(j\omega)| = 20\log_{10}2 - 10\log_{10}(1+\omega^2)$$
$$\angle L(j\omega) = -180(\omega T + \tan^{-1}\omega)/\pi$$

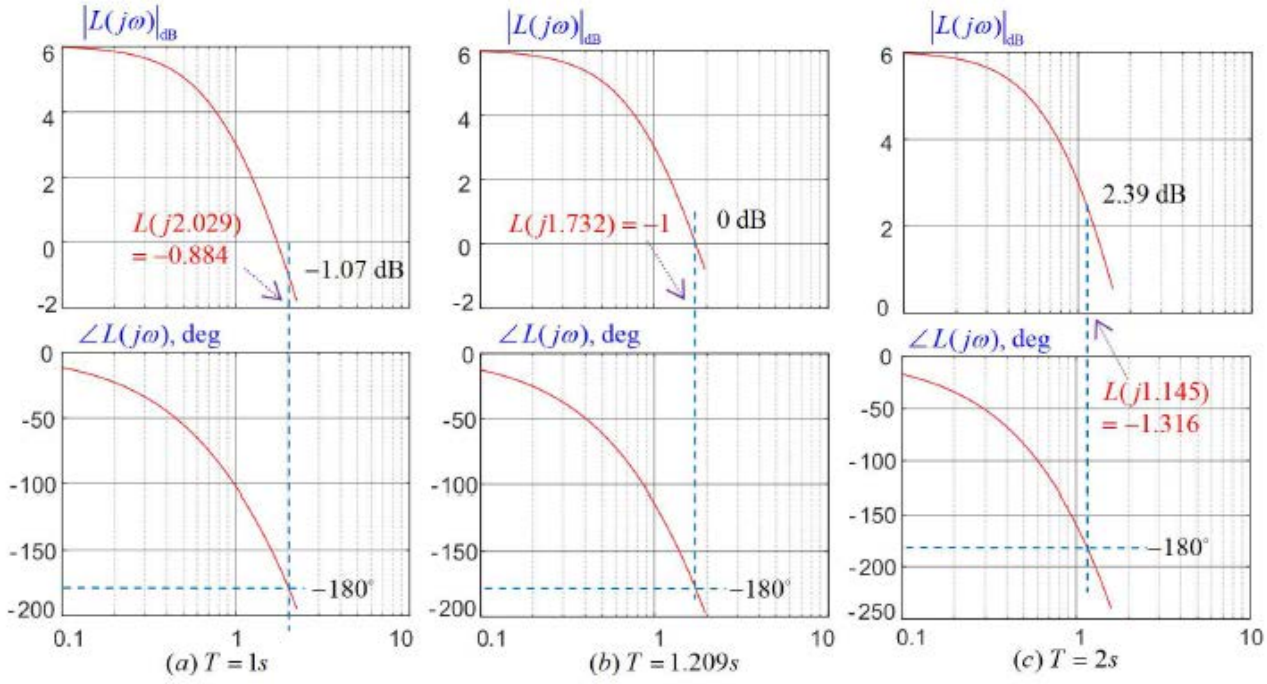

***Fig.* 14 Bode plot of $L(s) = \frac{2e^{-sT}}{s+1}$ with $T = 1\text{s}, 1.209\text{s}$, and 2s, respectively.**

The Bode plot of the loop transfer function $L(s)$ for three delay times, T = 1s, T = 1.209s, and T = 2s, are shown in *Fig*. 14(a), (b), and (c), respectively. These three Bode plot are associated with the three Nyquist plots shown in Fig.12(b), *Fig*.13(a), and *Fig*.13(b), respectively.

Note that the magnitude plots $|L(j\omega)|_{dB}$ versus ω are all identical, since the time delay only affects the phase. Larger delay time causes more phase shift.

The Bode plot for the case with delay time T = 1.209s is shown in Fig. 14(b). It shows that at the frequency ω = 1.732 rad/s, the phase is $\angle L(j1.732) = -180^{\circ}$ and the magnitude is $|L(j1.732)|_{dB} = 0_{dB}$, which means that the Nyquist plot of the $L(s)$ with delay time T = 1.209s intersects the real axis of the L-plane at the critical point $L(j1.732) = 1 \cdot e^{-j180^{\circ}}$, since 0 dB = 1. This delay time is the critical delay time T_c, for the system to be stable, the delay time must be smaller than T_c = 1.209s.

The Bode plot for the case with delay time T = 1s are shown in *Fig*.14(a). When the phase is -180°, the frequency is ω =2.029 rad/s, and the magnitude is $|L(j2.029)|_{dB} = -1.07$ dB, which means that $L(j2.029) = 0.884 \cdot e^{-j180^{\circ}}$, since $-1.07_{\text{dB}} = 0.884$. This 1.07dB = 1.131 gain margin means that the magnitude is allowed to increase by 1.131 times before the system becomes unstable. The definition of the stability gain margin will be officially defined in the next section.

The Bode plot for the case with delay time T = 2s are shown in *Fig*.14(c). When the phase is -180°, the frequency is ω = 1.145 rad/s, and the magnitude is $|L(j1.145)|_{dB} = 2.385$ dB, which means that $L(j1.145) = 1.316 \cdot e^{-j180^{\circ}}$, since 2.385dB =1.316. This -2.385 dB =0.76 gain margin means that the magnitude needs to decrease to 76% for the system to become stable.

Remark (Bode Plot and Nyquist Plot)

The Bode plot and the Nyquist plot are both important frequency-domain graphical tools for control systems design and analysis. Either one alone has its pros and cons, but they compensate for each other very well. The Nyquist plot, together with the Nyquist stability criterion, successfully address the stability issue of the infinite-dimensional systems and provide a meaningful measure of robust stability for control systems.

However, the Nyquist plot does not explicitly display the magnitude, the phase, and the frequency as clearly as the Bode plot. On the other hand, the information provided by the Bode plot alone is not enough for stability analysis because it only considers $s = j\omega$, the positive imaginary axis of the s-plane, not the whole Nyquist contour.

In some cases, the Bode plot can be a more precise and effective tool in control systems design. For a feedback control system with time delay, usually the system is assumed stable when the delay time is negligible. Then it is clear that the increase of the delay time can only make the system less stable. In this case, the Bode plot can be very effective in the design of a compensator to offset the influence of the time delay on the closed-loop system.

A Simple Compensation to Improve the Stability of a System with Time Delay

Ex 10: A Simple Compensator to Offset the Time Delay Influence on the Closed-loop System Stability

From the stability analysis of the system considered in Ex. 8 and Ex.9, we have learned that the closed-loop system will become unstable if the delay time is greater than the critical delay time T_c = 1.209s. For the case with delay time T = 2s, the closed-loop system is apparently unstable, as shown in the Nyquist plot in *Fig*.13(b) and the Bode plot in *Fig*.14(c).

By comparing the Bode plots in *Fig*.14(a) and *Fig*.14(c), we can see that the difference is in the sign of $|L(j\omega)|_{dB}$ at the phase-crossover frequency. When the sign is negative, as in *Fig*.14(a), $|L(j\omega)|_{dB} = -1.07$ dB, the closed-loop

system is stable. On the other hand, when the sign is positive, as in *Fig*.14(c), $|L(j\omega)|_{dB}$ = 2.39dB, the closed-loop system is unstable. Thus, it is possible to find a compensator to reduce the $|L(j\omega)|_{dB}$ to a negative value so that the closed-loop system will become stable.

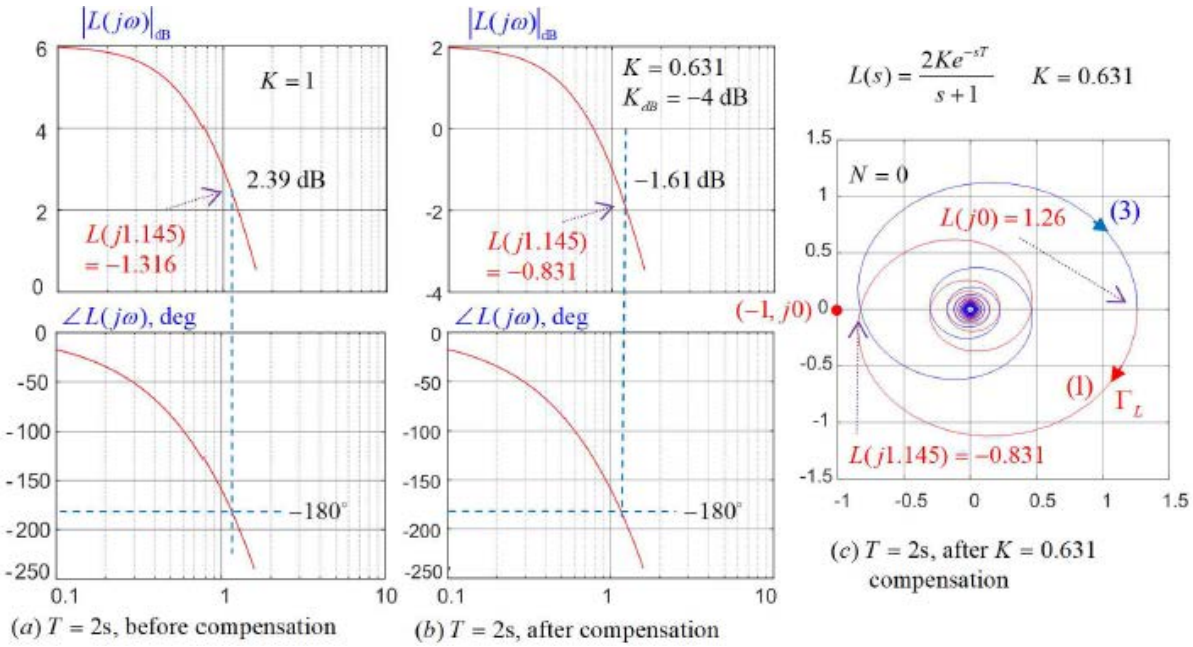

***Fig.* 15 Bode plot of $L(s)=\dfrac{2Ke^{-sT}}{s+1}$ with $T=2\text{s}$ and the proportional control $K=1$ and $K=0.631$, respectively.**

By inserting a simple constant proportional controller *K* to the loop transfer function so that $L(s)$ will be

$$L(s)=\frac{2Ke^{-sT}}{s+1}$$

Then the magnitude in dB and the phase in degree of $L(j\omega)$ will become

$$|L(j\omega)|_{dB}=20\log_{10}|L(j\omega)|=20\log_{10}2+20\log_{10}K-10\log_{10}(1+\omega^2)$$
$$\angle L(j\omega)=-180(\omega T+\tan^{-1}\omega)/\pi$$

Note that adding the proportional controller *K* only changes the magnitude while the phase remains unchanged. If $20\log_{10}K$ is chosen to be -4 dB, which is equivalent to *K* = 0.631, then the $|L(j\omega)|_{dB}$ magnitude plot curve will move

down by 4dB, as shown in *Fig*.15(b). Since the phase plot $\angle L(j\omega)$ remains the same, and the phase-crossover frequency is still at ω = 1.145 rad/s, the value of $|L(j\omega)|_{dB}$ at the phase-crossover frequency will be $|L(j1.145)|_{dB} = -1.61$ dB. Therefore, the insertion of the proportional control compensation with $20\log_{10} K = -4$ dB has transformed an unstable system to a stable system with a 1.61dB stability gain margin.

The Nyquist plot associated with the Bode plot of the compensated system is shown in *Fig*.15(c). The intersection of Γ_L with the negative real axis is now at $L(j1.145) = -0.831$, which is on the right-hand side of the critical point (marked as a red dot). Thus, the number of the clockwise encirclements of $(-1, j0)$ by Γ_L has changed from *N* = 1 to *N* = 0, and therefore the closed-loop system has become stable since the number of unstable closed-loop system poles is now *Z* = *N* + *P* = 0 + 0 = 0.

6.4 Robust Stability

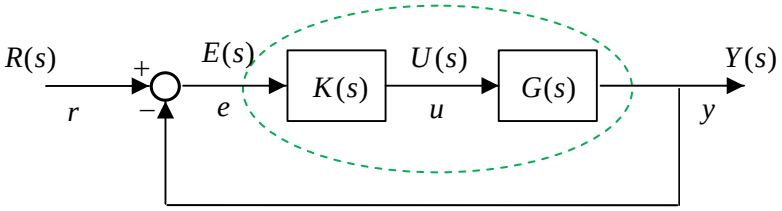

Fig. 7

Loop Transfer Function: $L(s) = G(s)K(s)$

Essential value of Nyquist's Theorem:

It allows us a direct method of evaluating stability robustness with respect to variations in the loop transfer function variation.

Gain Margin and Phase Margin for SISO Feedback Control Systems

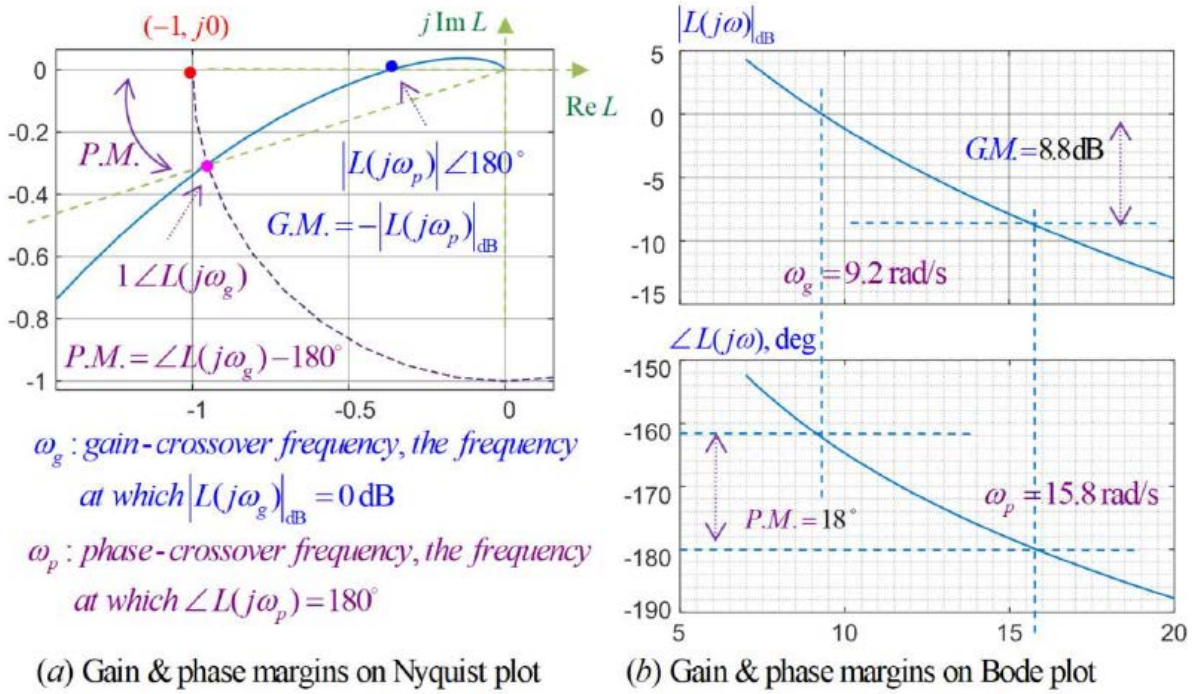

***Fig.* 16 Gain and phase margins for SISO feedback control systems**

6.4.1 Gain and Phase Margins

Reading Gain Margin from Nyquist Plot

In the partial Nyquist plot of $L(s)$ shown in *Fig*.16(a), the gain margin is determined by the position of the intersection (the blue dot) of the Nyquist image Γ_L (the blue curve) and the negative real axis. The intersection position is represented by the complex number on the *L*-plane:

$$\left|L(j\omega_p)\right|\angle 180^\circ$$

where ω_p is called the phase-crossover frequency at which the phase of $L(j\omega_p)$ is 180°. The gain margin is defined by the following equation:

$$GM = -\left|L(j\omega_p)\right|_{dB} = -20\log_{10}\left|L(j\omega_p)\right| \qquad \textbf{(9.47)}$$

If this intersection point is between the origin $(0, j0)$ and the critical point $(-1, j0)$ (the red dot), which means the intersection is on the right-hand side of $(-1, j0)$, then the magnitude $\left|L(j\omega_p)\right|$ will be less than 1 and the gain margin (GM) will be positive.

A closed-loop system with a positive gain margin does not mean it is stable. However, if the system is stable when the intersection point is between $(-1, j0)$ and $(0, j0)$, then the same system will continue to be stable as long as the intersection point remains inside the interval.

The gain margin is a good indication on how much gain variation is allowed for the system to stay stable. For example, if the intersection is at $(-0.1, j0)$ or $0.1\angle 180^\circ$, the gain margin will be

$$GM = -20\log_{10}0.1 = 20\ \text{dB}$$

and the system will remain stable if the system gain will not increase to ten times of its original gain. On the other hand, if the intersection point is at $(-0.8, j0)$ or $0.8\angle 180^\circ$, the gain margin will be

$$GM = -20\log_{10}0.8 = 1.94\ \text{dB}$$

and the system gain will only need to increase by 25% (or become 1.25 times of its original value) to move the intersection point to the other side of the critical point $(-1, j0)$ to destabilize the system. If the intersection point moves to the other side of the critical point $(-1, j0)$, the number of encirclements of $(-1, j0)$ by the Nyquist image contour will change; hence, the stability status of the closed-loop system will change according to the Nyquist stability criterion.

Therefore, the system will be more stable if the absolute value of gain margin is larger, or if the intersection point $|L(j\omega_p)|\angle 180^\circ$ is further away from the critical point $(-1, j0)$.

Reading Gain Margin from Bode Plot

Although the Nyquist plot clearly shows the intersection point of the Nyquist image Γ_L with the negative real axis, it does not reveal the phase-crossover frequency. Since the Bode plot explicitly show both the magnitude and the phase of $L(j\omega)$ as functions of the frequency, they provide more detailed information.

As defined, the gain margin is determined by the magnitude of $|L(j\omega_p)|\angle 180^\circ$. The phase-crossover frequency, ω_p, is the frequency at which the phase of $L(j\omega)$ is 180° or -180°. From the Bode plot shown in Fig.16(b), it is easy to see that the $\angle L(j\omega)$ phase curve intersects the -180° horizontal line when the frequency ω is the phase-crossover frequency ω_p. Draw a vertical straight line at the phase-crossover frequency, ω_p = 15.8 rad/s, and extend this line up to intersect the $|L(j\omega)|_{dB}$ magnitude curve. Then, the value of $|L(j\omega)|_{dB}$ at ω_p =15.8 rad/s can be read from the graph as $|L(j\omega_p)|_{dB} = -8.8\text{dB}$. Therefore, the gain margin is

$$GM = -|L(j\omega_p)|_{dB} = 8.8 \text{ dB}$$

Reading Phase Margin from Nyquist Plot

In the partial Nyquist plot of $L(j\omega)$, shown in *Fig*.16(a), the phase margin is determined by the intersection (the purple dot) of the Nyquist image Γ_L and the unit circle centered at the origin. The intersection position is represented by the complex number on the *L*-plane

$$1\angle L(j\omega_g)$$

where ω_g is called the gain-crossover frequency at which the magnitude of $L(j\omega_g)$ is one, or $\left|L(j\omega_g)\right|_{dB} = 0\text{dB}$. The phase margin is defined by the following equation:

$$PM = \angle L(j\omega_g) - 180^\circ$$

Just like the perturbation of the gain, the variation of the phase of the loop transfer function $L(s)$ can also destabilize a system. Recall that in Section 6.3.4, a time delay will cause a phase lag in the Nyquist plot of $L(s)$. A system with larger absolute value of phase margin will be more robust against the phase variations of the system.

Reading Phase Margin from Bode Plot

As defined, the phase margin is determined by the phase of $L(j\omega)$ at the gain-crossover frequency ω_g, the frequency at which the magnitude of $L(j\omega_g)$ is 1 or $\left|L(j\omega_g)\right|_{dB} = 0\text{dB}$. The first step is to find the gain-crossover frequency ω_g. From the Bode plot shown in *Fig*.16(b), it is easy to see that the intersection of the $\left|L(j\omega)\right|_{dB}$ curve with the 0 dB horizontal line on the magnitude plot occurs when the frequency ω is the gain-crossover frequency ω_g. Draw a vertical straight line at the gain-crossover frequency, ω_g = 9.2 rad/s, and extend this line down to the phase plot to intersect the $\angle L(j\omega)$ curve. The value of $\angle L(j\omega_g)$ at ω_g = 9.2 rad/s can be read from the phase plot that $\angle L(j\omega_g)$ is -162°. Therefore, the phase margin is *PM* = $-162^\circ - (-180^\circ) = 18^\circ$.

6.4.2 Effect of the Gain of Loop Transfer Function on Gain and Phase Margins

Ex 11: Stabilize an Originally Unstable System to a Desired Gain Margin

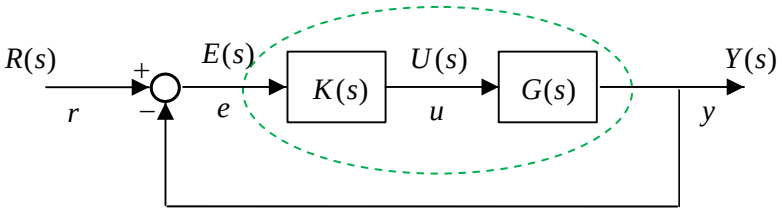

Fig. 7

Loop Transfer Function: $L(s) = G(s)K(s) = \dfrac{20000}{s^3 + 55s^2 + 250s}$

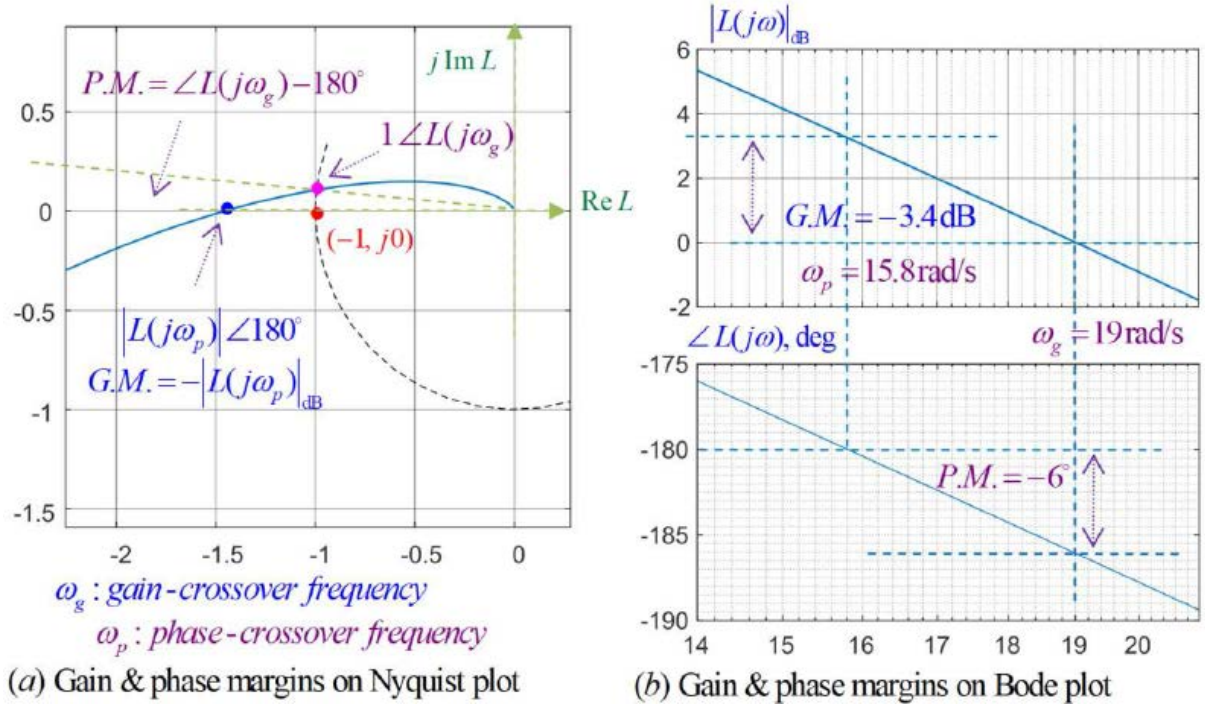

***Fig.* 17 The gain and phase margins of the unstable system in Ex. 11**

From the partial Nyquist plot and the Bode plot in *Fig.*17(a) and 17(b), respectively, we have found the gain and phase margins of the system as follows:

$$GM = -\left|L(j\omega_p)\right|_{\text{dB}} = -3.4 \text{ dB} \quad \text{where} \quad \omega_p = 15.8 \text{ rad/s}$$

$$P.M. = \angle L(j\omega_g) - 180^\circ = -6^\circ \quad \text{where} \quad \omega_g = 19 \text{ rad/s}$$

Note that the system has negative gain and phase margins, since the Nyquist image Γ_L intersects the negative real axis at the left-hand side of the critical point $(-1, j0)$. In general, a system with negative gain or phase margin does not mean the closed-loop system is unstable. The information given by the partial Nyquist plot and the Bode plot is not enough to determine if the closed-loop system is stable.

However, it is quite straightforward to check the closed-loop stability by solving the three roots of the characteristic equation or using the Routh-Hurwitz criterion, or the Nyquist stability criterion based on the complete Nyquist plot. The system is indeed unstable, but both the gain and phase margins are small.

A gain margin of -3.4 dB means that it only requires a small gain reduction of $L(s)$ to 67% of its original gain to stabilize the closed-loop system.

Assume the loop transfer function $L(s)$ structure is slightly modified to

$$L(s) = \frac{20000K}{s^3 + 55s^2 + 250s}$$

where *K* is a constant gain to be designed. The system is the same as the original one if *K* = 1.

In general, this *K* can be a function of *s*, or $K(j\omega)$ is a function of frequency ω, so that the system can be designed to satisfy multiple design objectives like robust stability, disturbance reduction, and control-input constraints.

Here, we will assume *K* is just a constant parameter to be determined so that a robust stability objective can be achieved.

Now the closed-loop system is unstable with gain margin -3.4 dB and phase margin -6°. We would like to design a simple constant controller *K* so that the closed-loop system is stable with gain margin improved to 14.6 dB.

Since the change of *K* will not affect the phase, the phase plot will remain the same. From the Bode plot in *Fig*.18(b), it can be seen that the gain and phase margins will improve if the $|L(j\omega)|_{dB}$ curve is moved down on the magnitude plot while the phase plot remains unchanged.

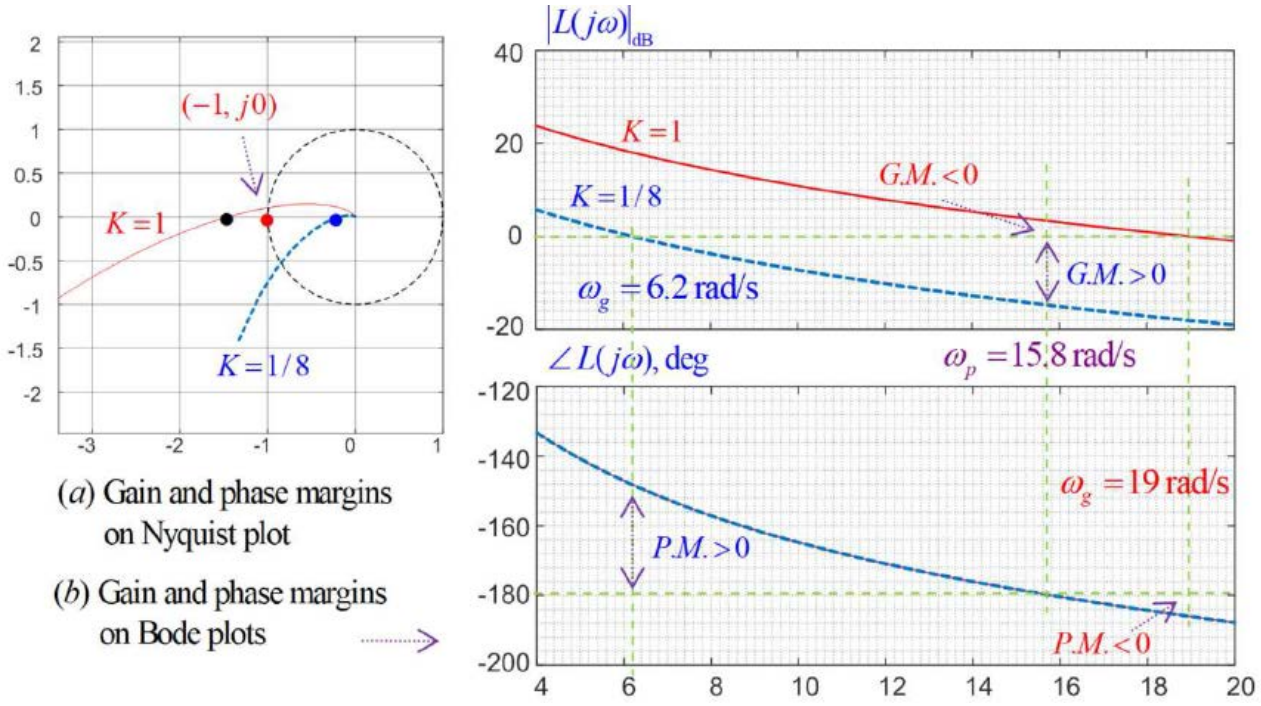

***Fig.* 18 Illustration of reducing *K* to move down the $|L(j\omega)|_{dB}$ curve to improve the gain and phase margins of an originally unstable closed-loop system in Ex.11.**

The graphs in *Fig.*18(a) and (b) show the differences between the original system (with *K* = 1) and the modified system (with *K* = 1/8) in the Nyquist plot and in the Bode plot. The Nyquist plot shows that the Nyquist image Γ_L has moved its intersection point with the negative real axis from the black dot position, crossing over the red dot critical point $(-1, j0)$, to become stable toward the blue dot position.

The Nyquist plot shows clearly that an obvious robust stability improvement has been achieved, but it does not reveal the details quantitatively.

The Bode plot shows clearly that if the objective is to achieve a gain margin of 14.6 dB, then *K* needs to be reduced to a level so that the $|L(j\omega)|_{dB}$ curve can move down by 18 dB on the magnitude plot. The 18 dB reduction of gain is approximately equivalent to reducing *K* from 1 to 1/8.

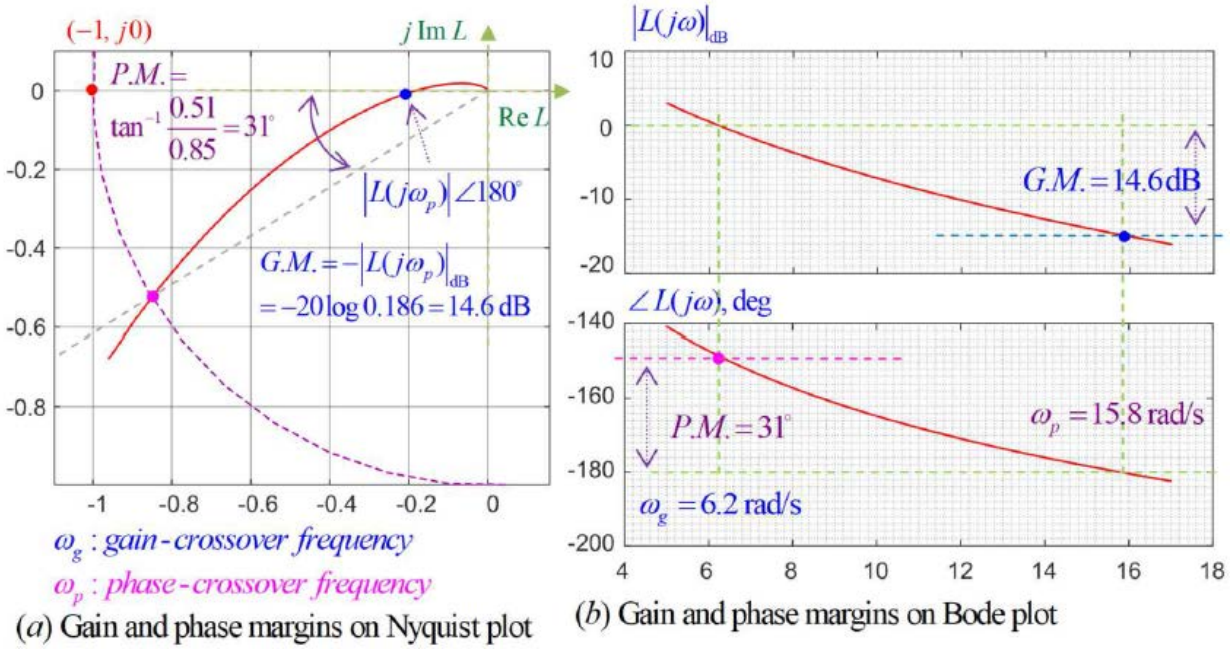

***Fig.* 19 Illustration of reducing *K* to from 1 to 1/8 to improve the gain margin by 18 dB and the phase margin by 37° in Ex. 11.**

With K = 1/8, the Nyquist plot and the Bode plot have been modified to those shown in *Fig.*19(a) and (b), respectively. It can be seen that the phase-crossover frequency is still at ω_p = 15.8 rad/s, but due to the 18 dB reduction of $|L(j\omega)|_{dB}$, the gain margin has improved from −3.4 dB to 14.6 dB. Although the phase plot remains unchanged, the gain-crossover frequency has changed from ω_g = 19 rad/s to ω_g = 6.2 rad/s, and the phase margin has improved from -6° to 31°.

In the following example, we will revisit the system considered in Ex. 7. The system has a double-crossing Nyquist image that intersects the negative real axis twice. According to Nyquist stability criterion, the closed-loop system will be stable when these two intersections are at the opposite sides of the critical point $(-1, j0)$. Furthermore, the gain margins are determined by the two intersection positions. The gain margin for the intersection on the right is positive while the other has a negative gain margin.

Ex 12: A System with Double-crossing Nyquist Image Has Positive and Negative Gain Margins at the Same Time

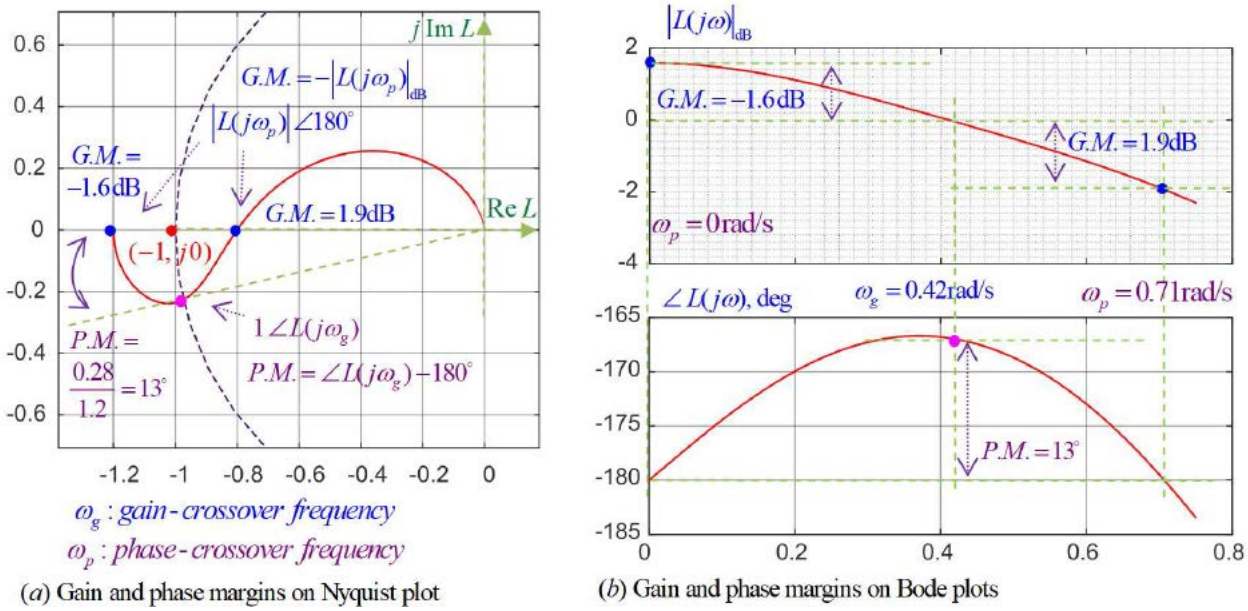

(*a*) Gain and phase margins on Nyquist plot (*b*) Gain and phase margins on Bode plots

***Fig.* 20 Revisit the double-crossing Nyquist image of Ex.7 that has positive and negative gain margins at the same time.**

The system considered in Ex. 7 has a double-crossing Nyquist image, as shown in *Fig.*11. Its loop transfer function is

$$L(s) = \frac{0.6K}{(s-0.5)(s^2+s+1)}$$

A partial Nyquist plot and the Bode plot of $L(s)$ with K = 1 are shown in *Fig.*20(a) and (b), respectively. Note that the Nyquist image Γ_L intersects the negative real axis of the L-plane at the following two points:

$$L(j0) = -1.2 \quad \text{and} \quad L(j\sqrt{0.5}) = -0.8$$

It has been shown in Ex. 7 that the system is stable. According to the definition of gain and phase margins, the system has a phase margin $PM = 13^\circ$ but has two gain margins

$$GM_1 = -20\log_{10}0.8 = 1.9382 \text{ dB} \quad \text{and} \quad GM_2 = -20\log_{10}1.2 = -1.5836 \text{ dB}$$

The positive gain margin on the right is $GM_1 = 1.9382\,\text{dB}$. It means that the gain of the loop transfer function *K* is allowed to increase to *K* = 1.25 without destabilizing the closed-loop system.

On the other hand, the negative gain margin $GM_2 = -1.5836\,\text{dB}$ indicates that the closed-loop system can stay stable as long as *K* is not reduced to below *K* = 5/6. In other words, the closed-loop system is stable if and only if

$$5/6 < K < 1.25$$

Note that the stability range of *K* derived in terms of the two gain margins is consistent with the inequality in Ex.7, which was found based on the Nyquist stability criterion.